1988

Microstructural Evolution by Continuous Recrystallization in a Superplastic Al-Mg Alloy

Hales, S.J.; McNelley, T.R.

Pergamon Press plc.

Hales, S. J., and T. R. McNelley. "Microstructural evolution by continuous recrystallization in a superplastic Al-Mg alloy." Acta Metallurgica 36.5 (1988): 1229-1239. http://hdl.handle.net/10945/62224

Acta metall. Vol. 36, No. 5, pp. 1229–1239, 1988
Printed in Great Britain

0001-6160/88 $3.00 + 0.00
Pergamon Press plc

MICROSTRUCTURAL EVOLUTION BY CONTINUOUS RECRYSTALLIZATION IN A SUPERPLASTIC Al–Mg ALLOY

S. J. HALES and T. R. McNELLEY
Materials Engineering Group, Department of Mechanical Engineering, Code 69, Naval Postgraduate School, Monterey, CA 93943–5000, U.S.A.

(*Received* 9 *March* 1987; *in revised form* 7 *September* 1987)

Abstract—The boundary misorientations in an Al–10 Mg–0.1Zr (wt%) alloy, thermomechanically processed by rolling at 573 K (300°C), were determined both in annealed and in superplastically deformed conditions. A high initial dislocation density in as-rolled material, which obscured any underlying structure, rapidly transformed into a well-defined structure containing boundaries. After annealing for 600 s at 573K, boundaries with misorientations of 1–5° were observed. With further annealing (3000 s), misorientations did not change appreciably and were measured to be 2–7°. Such time represents that necessary to equilibrate at 573K prior to tension testing at that temperature. The material exhibits superplasticity from the onset of deformation and after 100% strain, misorientations were observed to increase to 20–30°. It was concluded that boundaries of such initial misorientations can support superplastic deformation mechanisms including grain boundary sliding.

Résumé—Nous avons déterminé les désorientations des joints dans un alliage d'aluminium à 10% en poids de magnésium et 0,1% en poids de zirconium elaboré par traitement thermomécanique (laminage à 573 K), l'alliage étant recuit ou déformé superplastiquement. La forte densité initiale de dislocations qui caractérise le matériau brut de laminage, et qui cache toute la structure sous-jacente, se transforme rapidement en une structure bien définie comportant des joints. Après un recuit de 600 s à 573 K, des joints de désorientation comprise entre 1 et 5° apparaissent. Pour un recuit ultérieur pendant 3000 s, les désorientations ne varient pas beaucoup et restent comprises entre 2 et 7°. Un tel temps de recuit représente le temps nécessaire à l'équilibre à 573 K avant l'essai de traction à cette température. Le matériau présente un comportement superplastique dès les premiers stades de la déformation, et après une déformation de 100%, les désorientations augmentent jusqu'à atteindre 20 à 30°. Nous en concluons que les joints qui possèdent au départ de telles désorientations peuvent se déformer par des mécanismes de déformation superplastique incluant le glissement intergranulaire.

Zusammenfassung—An ausgeheilten und an superplastisch verformten Proben der Legierung Al–10 Mg–0,1 Zr (in Gew.-%), die thermomechanisch durch Walzen bei 573 K behandelt worden waren, wurden die Fehlorientierungen an Korngrenzen gemessen. Die hohe Versetzungsdichte, die sich in den gewalzten Proben fand und die Analyse der Fehlorientierungen behinderte, wandelte sich rasch in eine wohldefinierte Struktur mit Korngrenzen um. Nach Asheilen bei 573 K für die Dauer von 600 s finden sich Korngrenzen mit Fehlorientierungen zwischen 1 bis 5°. Bei längerem Ausheilen (3000 s) ändern sich die Fehlorientierungen nicht wesentlich, sie liegen zwischen 2 und 7°. Diese Ausheilzeiten wurden als diejenigen angenommen, die für eine Gleichgewichtseinstelung des Materials vor dem Zugversuch nötig sind. Die Proben verformen sich von Beginn an superplastisch; nach einer Dehnung von 100% betragen die Fehlorientierungen 20–30°. Daraus läßt sich folgern, daß die Korngrenzen mit den vergleichsweise geringen Fehlorientierungen die superplastischen Verformungsmechanismen einschließlich der Korngrenzgleitung unterstützen können.

1. INTRODUCTION

Wrought superplastic Al alloys exhibit a highly strain-rate sensitive flow stress when deformed at an approximate homologous temperature of $0.9\,T_m$ [1, 2]. Often, the stress vs strain-rate relationship is observed to be sigmoidal when data are plotted on double logarithmic coordinates [1–5]. Maximum ductilities are usually obtained at the strain rate corresponding to the maximum value of the strain-rate sensitivity coefficient, m ($=\mathrm{d}\ln\sigma/\mathrm{d}\ln\dot{\varepsilon}$), [4–7] and it has been demonstrated both experimentally [8] and analytically [9] that increased ductility can be correlated with an increase in m.

The value of m depends on mechanisms determined by the microstructure and deformation conditions and is reported to be ~ 0.5 for many superplastic materials [3–6]. It is, therefore, of interest to identify the microstructural features responsible for the strain-rate dependence of the flow stress. Most authors are in agreement that grain boundary sliding (GBS) is the dominant deformation mechanism during superplastic flow [3, 4, 6]. The microstructural prerequisites for such a mechanism are a fine, equiaxed grain size, generally below 10 μm and mobile high-angle boundaries [3, 4, 6]. The latter requirement reflects the need for accomodation of GBS by diffusion or diffusion-controlled (e.g. dislocation climb) processes [3–6]. These diffusional processes, in

turn, require boundaries capable of emission and absorption of vacancies.

Methods of achieving fine-grain superplasticity in wrought Al–Zn–Mg–Cu (7XXX) alloys have centered around controlled thermomechanical processing (TMP) [2, 7, 10, 11]. The microstructural prerequisites for superplasticity have been realized using subsequent heat treatments to transform a highly deformed microstructure to a fine-grained microstructure via a discontinuous recrystallization process. This mechanism is characterized by the nucleation and growth of new, strain-free grains involving the formation and migration of high-angle boundaries [12]. Bimodal distributions of second phase particles are desirable for achieving grain refinement [7]; the coarser particles ($\sim 1\ \mu$m) promote high-angle boundary formation while the finer particles (20–50 nm) restrict high-angle boundary migration.

An alternative approach has been developed for producing fine-grained Al–Cu–Zr (SUPRAL) alloys capable of sustaining superplastic deformation [1]. No recrystallization heat treatments are used prior to elevated temperature deformation and the materials exhibit a superplastic response while in an apparently nonrecrystallized condition [13]. Nes [14] has suggested that the microstructures transform by a continous recrystallization process during the initial stages of hot deformation. This mechanism is characterized by the development of moderate misorientations between adjacent dislocation-free regions in the absence of high-angle boundary migration [7, 12]. Dislocations rearrange to such an extent that the resultant boundary misorientations are larger than commonly expected for well-defined subgrain structures. The mechanical response of these alloys has been interpreted as evidence for GBS in microstructures where the average boundary misorientation is 5–7° [15]. Further work by Bricknell and Edington [16] on these alloys has provided evidence for dislocation motion during superplastic deformation at maximum m-value. These observations have been interpreted in terms of accomodation of GBS by dislocation deformation processes.

Research on TMP of Al–Mg alloys containing 10 wt% Mg has revealed that the materials also behave in a superplastic manner while in a deformed, nonrecrystallized condition [17–20]. Superplastic elongations up to 500% have been obtained at 573K (300°C) and $2–5 \times 10^{-3}\ s^{-1}$ strain rate [18, 19]. The homologous temperature, $0.7\ T_m$, is considerably lower than generally reported for wrought Al alloys and the strain-rate higher by an order of magnitude. Since the usual microstructural prerequisites were not realized and nucleation and growth of new grains was not observed, it was proposed that a continuous recrystallization mechanism yielding a fine-grained (2–5 μm) microstructure at 573 K would account for the results [19]. It was also possible to correlate apparent strain hardening during superplastic flow with grain growth and a decrease in m-value [19]. In contrast, material experiencing the same TMP but exposed to a final recrystallization heat treatment, prior to elevated temperature testing, did not exhibit superplasticity at 573 K [18]. Thus, the objective of this investigation is to quantify the microstructural evolution pertaining to the superplastic response of these Al–Mg alloys when deformed at 573K.

Table 1. Alloy composition (wt%)

Mg	Zr	Si	Fe	Ti	Be	Al
9.89	0.09	0.02	0.02	0.01	0.0003	Balance

2. EXPERIMENTAL

2.1. Material processing

The composition of the alloy studied in this investigation is given in Table 1; the material was provided in the form of a direct-chill cast ingot by Alcoa Technical Center, Alcoa Center, Pa. Essential features of the TMP are [17]: solution treatment and hot working by upset forging at 713K (440°C), well above the Mg-solvus temperature, ~643K (370°C); quenching; reheating and rolling at 573K to a final reduction of 92% ($\epsilon_{true} = 2.3$).

Elevated temperature mechanical properties were obtained using samples with the following gage dimensions: 12.7 mm length; 5.1 mm width; 2.0 mm thickness; and 1.6 mm shoulder radius. These were machined from the as-rolled material with tensile axes parallel to the rolling direction. Tension testing at 573K was accomplished utilizing constant crosshead speeds and the data were reduced to true stress versus true strain plots for the various initial strain-rates [17]. These data were then corrected to compensate for the decrease in true strain-rate with increasing strain; details of this compensation method have been given previously [19].

Separate sample geometries were employed for detailed assessment of the effects on microstructure of both time-at-temperature and deformation. Static annealing treatments at 573 K, to stimulate warm-up to the elevated test temperature, were conducted on small samples (20 mm × 20 mm), taken from the as-rolled material, utilizing neutral salt baths for accurate control of heating time and temperature. Larger tension samples with gage dimensions of 50.8 mm length, 20.3 mm width, 3.8 mm thickness and 6.4 mm shoulder radius were machined to study the effects of simulated superplastic forming. These were deformed at 573K at a nominal strain-rate of $1.67 \times 10^{-2}\ s^{-1}$, corresponding to the approximate strain-rate at which peak ductilities were obtained from the initial testing. The same testing procedures were followed, including the 2700–3600 s heating time prior to the commencement of straining. These samples were deformed to a nominal strain of 100%, a strain considerably less than the fracture strain, and which proved to be especially convenient for subsequent microstructural analyses. The samples were cooled in

air at the completion of deformation and sectioned so that both the undeformed grip sections and deformed gage sections could be examined.

2.2. Microstructural analysis

Transmission electron microscopy (TEM) studies were conducted on specimens removed from bulk material such that foil normals were parallel to the sheet normal direction. Electrothinning was accomplished utilizing a 25% nitric acid in methanol solution at 253K (−20°C) and 15V. Most of the microstructural evaluation was conducted on a JEOL 100CX operating at 120kV. In addition, the convergent beam electron diffraction (CBED) capability of the Phillips EM430 operating at 300kV was utilized for boundary misorientation determinations. Orientation studies on the constituent grains in microstructures pertaining to the various material conditions were conducted using CBED. In each case a reference grain with [011] oriented parallel to the beam direction was selected and CBED patterns obtained from the neighboring grains without reorienting the foil. The relative grain orientations were then determined by identifying the positions of the various CBED patterns in Kikuchi space. These data were plotted on stereographic triangles to effectively represent localized pole figures with a [011] oriented reference grain. In instances where the orientations of adjacent grains were determined, the misorientation angle of the common boundary was calculated.

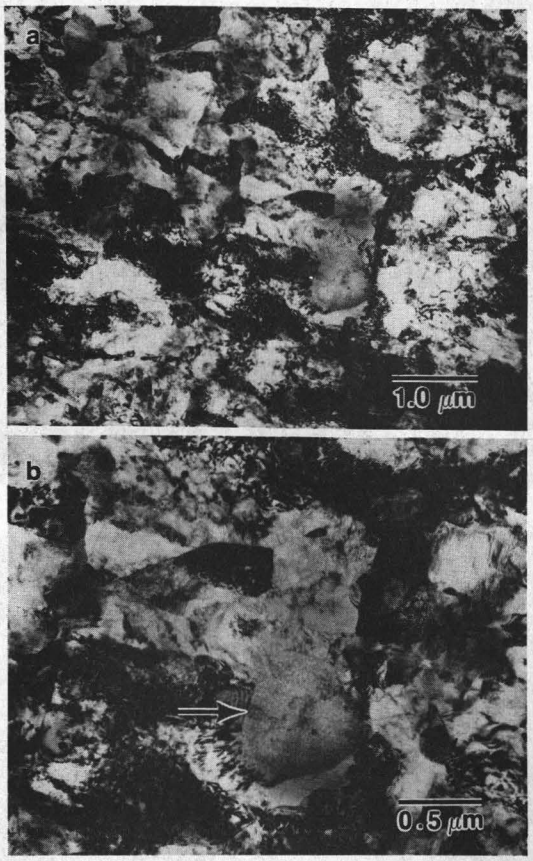

Fig. 1. Bright field electron micrographs of the Al–10 Mg–0.1 Zr (wt%) alloy, rolled at 573K (300°C) to a strain of 2.3 (92% reduction), showing (a) the tangled dislocation structure and (b) a β (Al_8Mg_5) particle (arrowed).

3. RESULTS

The microstructure typical of as-rolled material is shown in Fig. 1. Warm-rolling to a true strain of 2.3 (~92% reduction) at 573K has produced a very high dislocation density which obscures the underlying structure of the material. The β phase (an intermetallic based on Al_8Mg_5) is present as discrete particles ~1 μm in size, Fig. 1(b), distributed throughout the microstructure. It was also observed in areas where prior grain boundaries from the solution-treated condition were identifiable that they were heavily decorated with β phase.

This microstructure is changed dramatically by a brief (120 s) heat treatment at 573K as seen in Fig. 2.

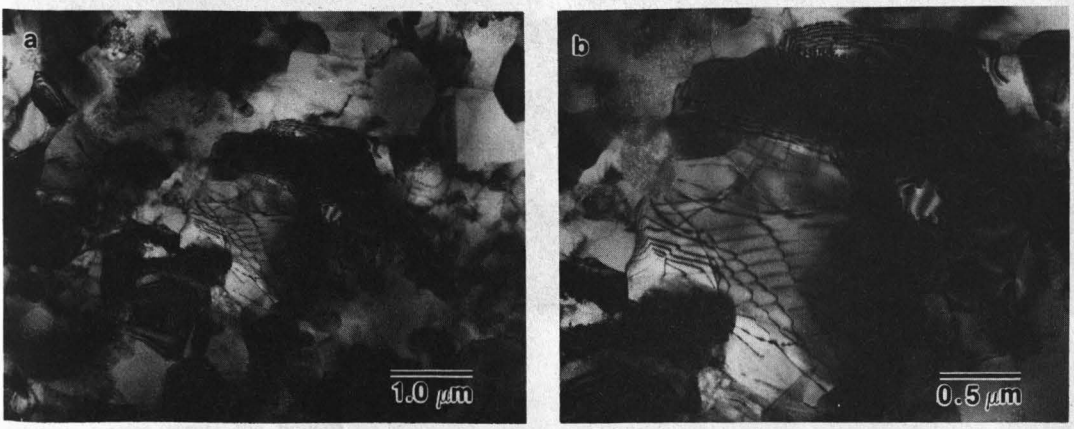

Fig. 2. Bright field electron micrographs illustrating the effect of 120 s annealing at 573K (300°C) on the structure of the rolled condition of Fig. 1 showing (a) rapid recovery and emergence of well-defined structure and (b) dislocation structures associated with boundaries.

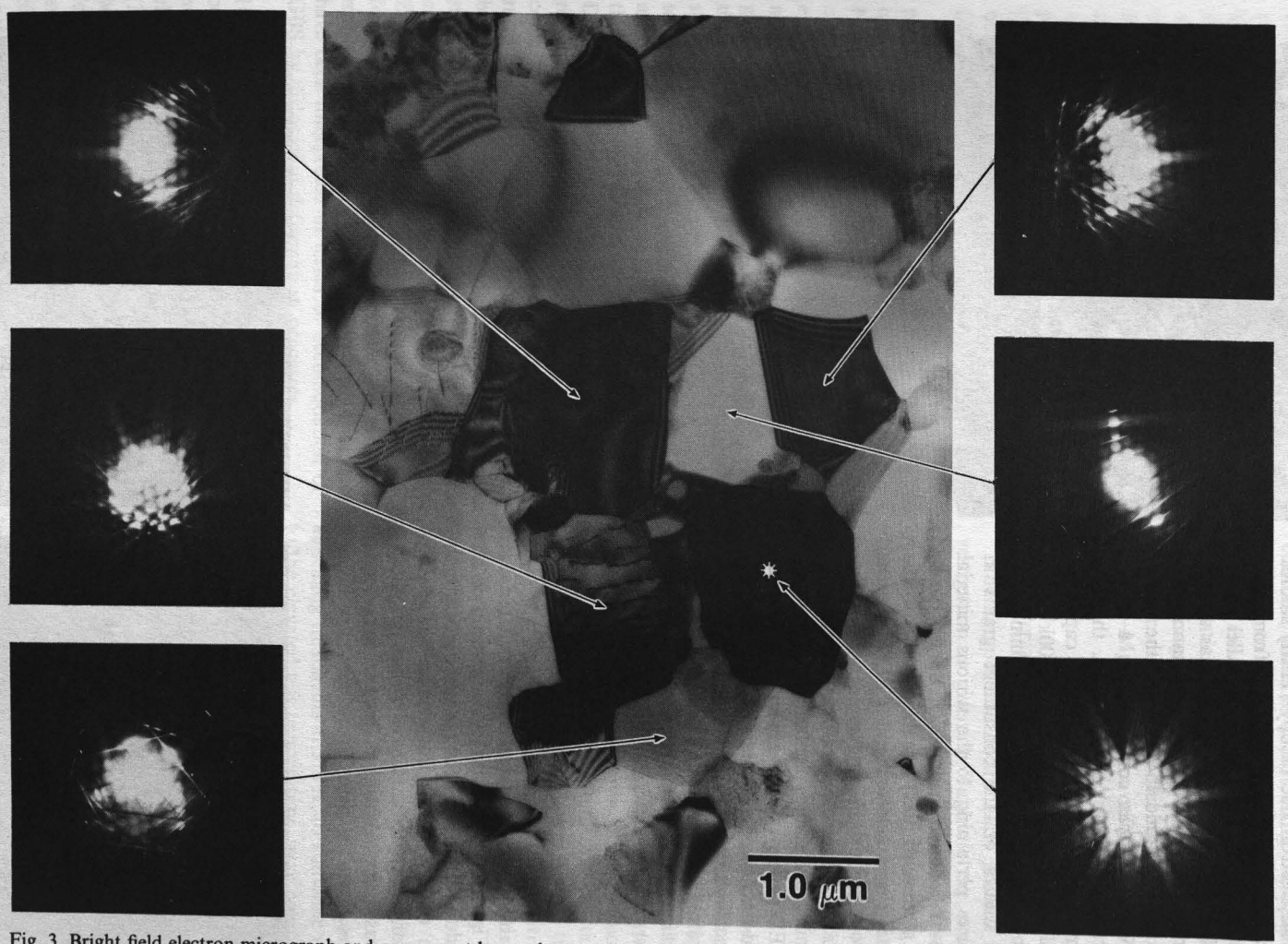

Fig. 3. Bright field electron micrograph and convergent beam electron diffraction (CBED) patterns indicating orientation variations between adjacent dislocation-free regions in material rolled at 573K (300°C) and then annealed for 600 s at the same temperature. The reference grain indicated (*) is oriented with [011] parallel to the beam direction (B).

The tangled dislocation networks in the as-rolled material have transformed rapidly into a better-defined substructure, with the β phase residing at subgrain boundaries. The majority of subgrains are 1–2 μm in size and contain few dislocations. There are, however, larger subgrains present containing a considerable number of dislocations which appear to be in the process of forming regular arrays, Fig. 2(b). Further annealing at 573K for 600 s produces a microstructure in which most of the dislocations have been absorbed into boundaries as seen in Fig. 3. The structure has coarsened somewhat and the CBED patterns obtained indicate that misorientations across the constituent boundaries have developed. Detailed examination of these data reveal that the boundary misorientations are 1–5° but there are isolated examples of considerably higher values. The values of these misorientations are summarized in Fig. 4, which indicate that the structure consists of boundary misorientations ranging from those characteristic of subgrains to those characteristic of grains.

As noted previously, mechanical test samples require 2700–3600 s to equilibrate at the test temperature, 573K. Thus, the grip section of a test sample deformed to 100% at $10^{-2}\,s^{-1}$ strain-rate will have experienced the equivalent of a 2700–3600 s annealing treatment. The microstructure from such a grip section, shown in Fig. 5, has the appearance of a fully recrystallized grain structure. Some of the grains are traversed by subgrain boundaries, an example of which is shown in Fig. 5(b). The accompanying weak beam micrograph, Fig. 5(c), reveals the individual, regularly-spaced dislocations comprising the subgrain boundary within an otherwise dislocation-free grain. It is also apparent that the β-phase has not coarsened appreciably and resides at grain boundary triple points. The mottled effect on the β, evident in Fig. 5, has been identified as a surface layer resulting from electropolishing during TEM specimen preparation.

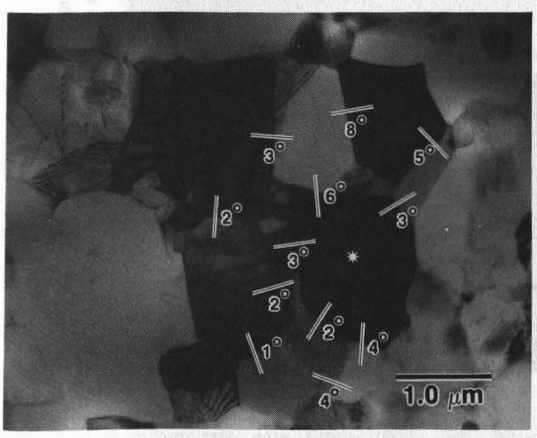

Fig. 4. Summary of the data from Fig. 3, with misorientation angles across the boundaries indicated. These angles were calculated from the relative misorientations of the neighboring grains with respect to the [011] direction of the reference grain (*). Most values are in the range 1–5°.

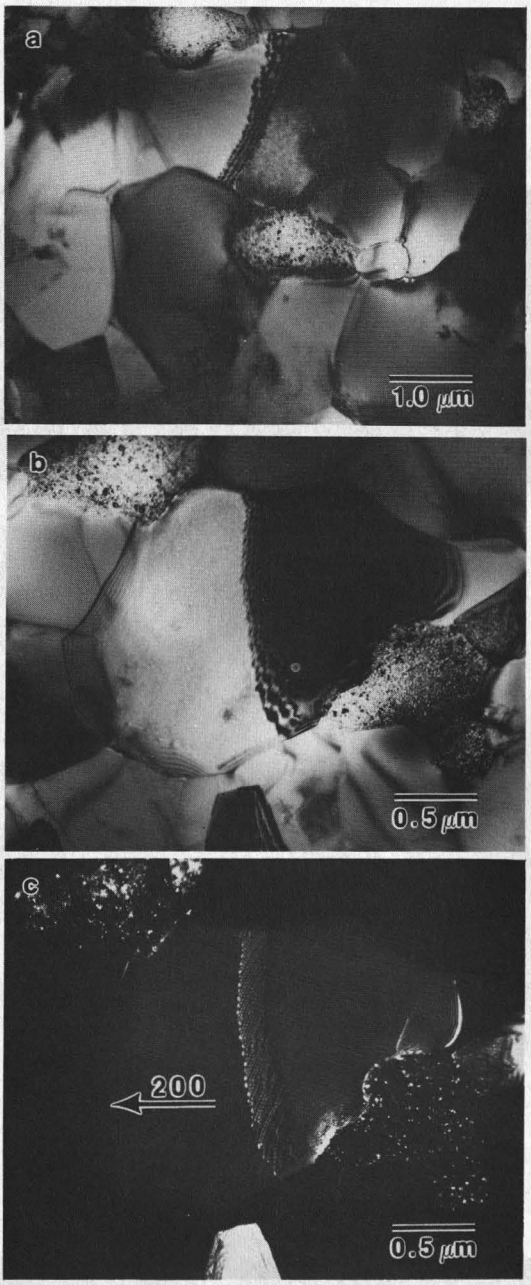

Fig. 5. Electron micrographs from the grip section of an elevated temperature test sample which has experienced approximately 3000 s total time at 573 K (300°C); (a) bright field showing fine grain structure with intergranular β precipitates; (b) bright field image showing a typical grain traversed by a subgrain boundary; (c) corresponding weak beam dark field (WBDF) image ($g/3g$, $B = [011]$) showing the spacing of dislocations comprising the subgrain boundary.

Figure 6 represents the misorientation data obtained from this grip section. The micrograph reveals that the grain size has changed little when compared to shorter annealing times, namely 1–3 μm. This microstructure effectively represents the condition of the material at the onset of deformation in a typical elevated temperature tension test. Values of bound-

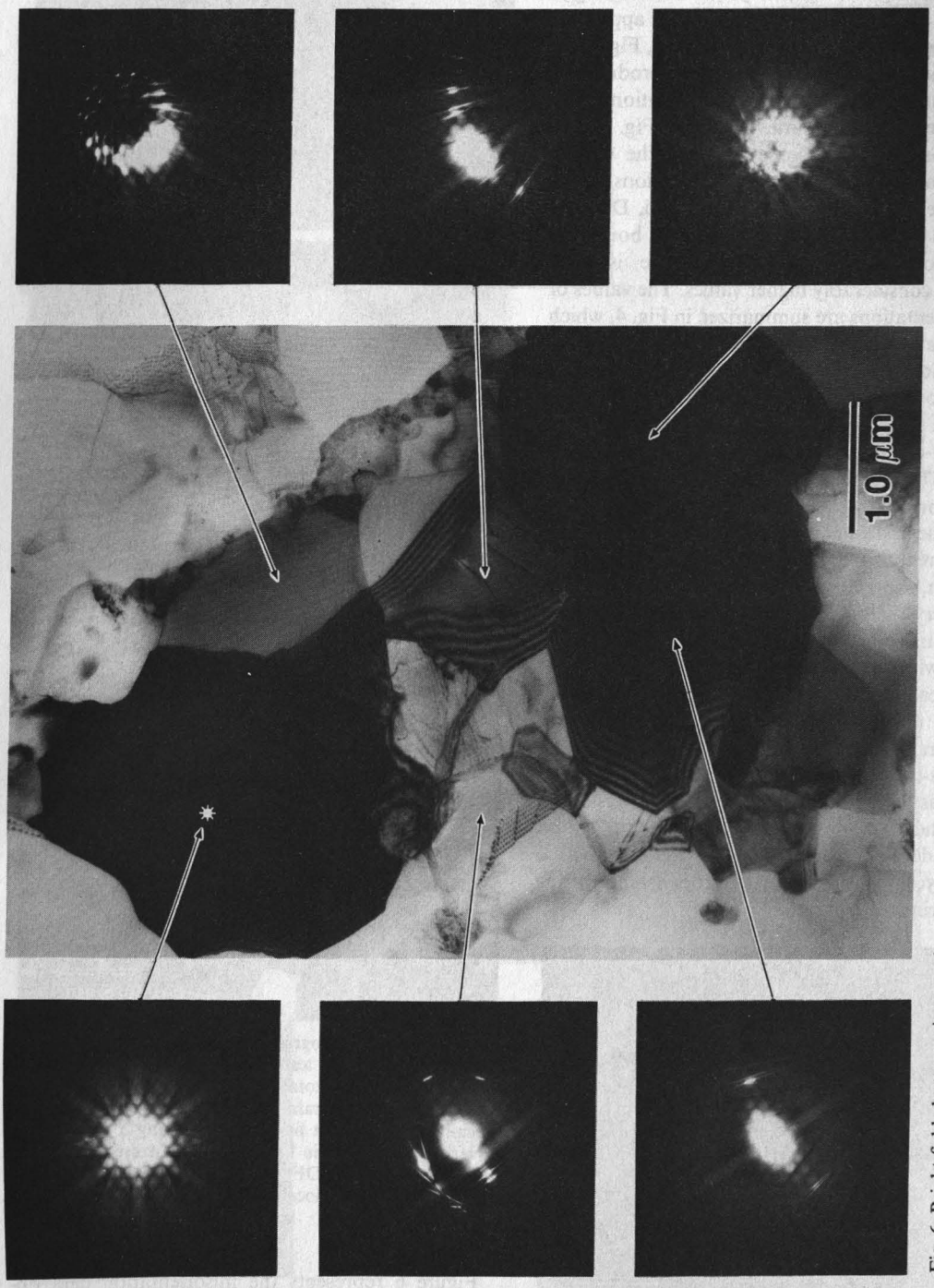

Fig. 6. Bright field electron micrograph and CBED patterns indicating orientation variations between adjacent grains in material from the grip section sample of the previous figure. The reference grain (*) is oriented with [011] parallel to *B*; misorientations are similar to those observed for shorter annealing times (Fig. 3).

Fig. 7. Summary of the data from Fig. 6; misorientation angles, calculated from the orientation of neighboring grains relative to the reference grain (*), are shown. The range of values is similar to that observed in material which has experienced shorter annealing times (Fig. 4).

ary misorientations are summarized in Fig. 7 and can be seen to be similar to these documented in Fig. 4, i.e. 2–7°. Also present in this micrograph is an example of a prior grain boundary from the initially solution-treated condition, as indicated by the arrows. This boundary is decorated with an approximately continuous string of β precipitate particles.

The mechanical property data for the elevated temperature testing is shown in Fig. 8, and is the same data reported previously for this material. Maximum ductilities are achieved between strain-rates of 10^{-3} and $10^{-2}\,s^{-1}$, where maximum m-values are obtained,

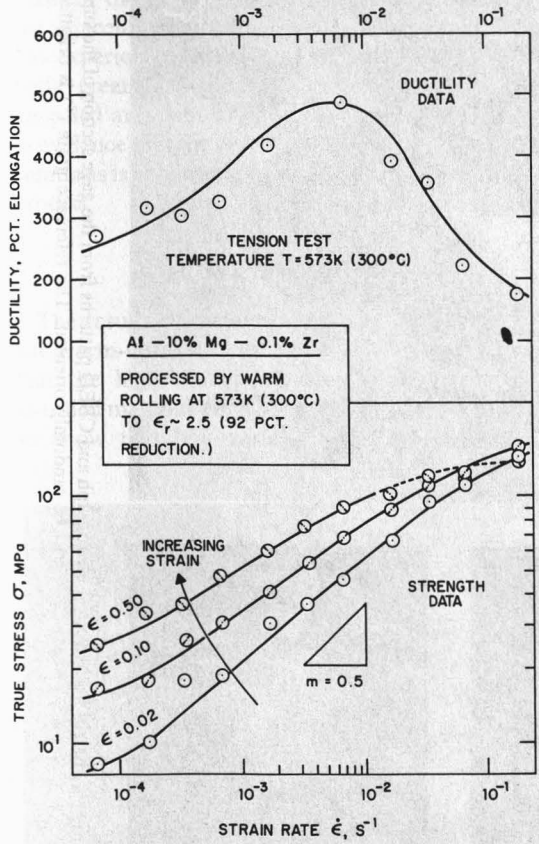

Fig. 8. Mechanical test data from this alloy, obtained from constant crosshead speed tension tests at 573K (300°C). The stress versus strain rate data (lower plot) have been corrected for the decrease in strain-rate with strain, the rate sensitivity coefficient, m, is largest at small strains and decreases with deformation due to microstructural coarsening. The peak ductility corresponds to the rate ($\sim 10^{-2}\,s^{-1}$) for peak m-value.

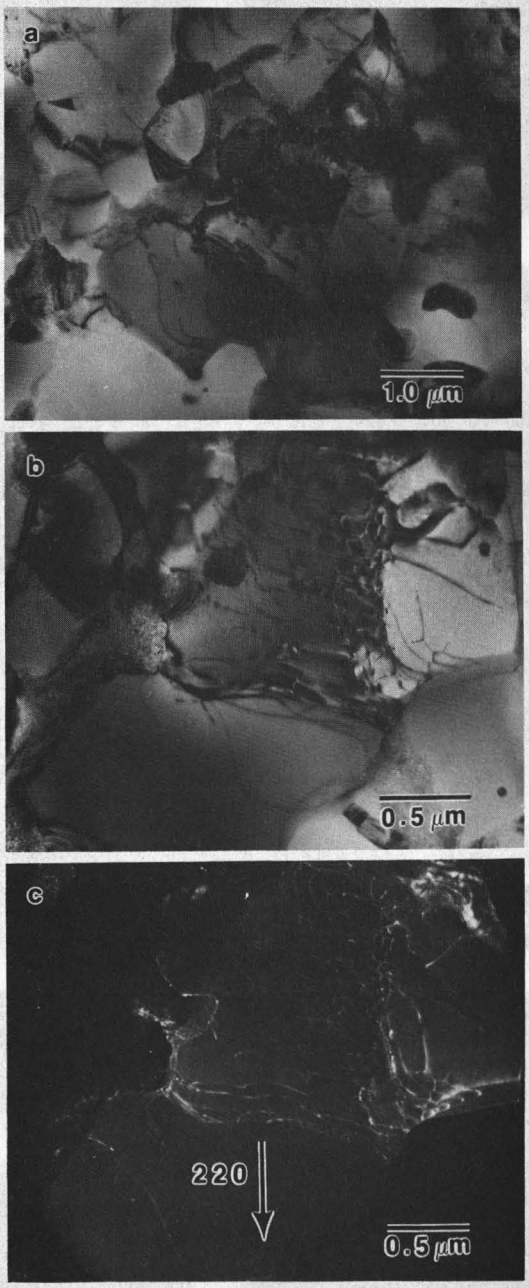

Fig. 9. Electron micrographs of material deformed to 200% elongation at 573K (300°C) and a strain-rate of $10^{-2}\,s^{-1}$; (a) bright field image showing the slightly elongated grain structure; (b) bright field image showing a typical distorted grain; (c) corresponding WBDF image ($g/3g$, $B = [011]$) showing the dislocation structure within the grain. The strain-rate is that at which peak ductilities were achieved in this material (Fig. 8).

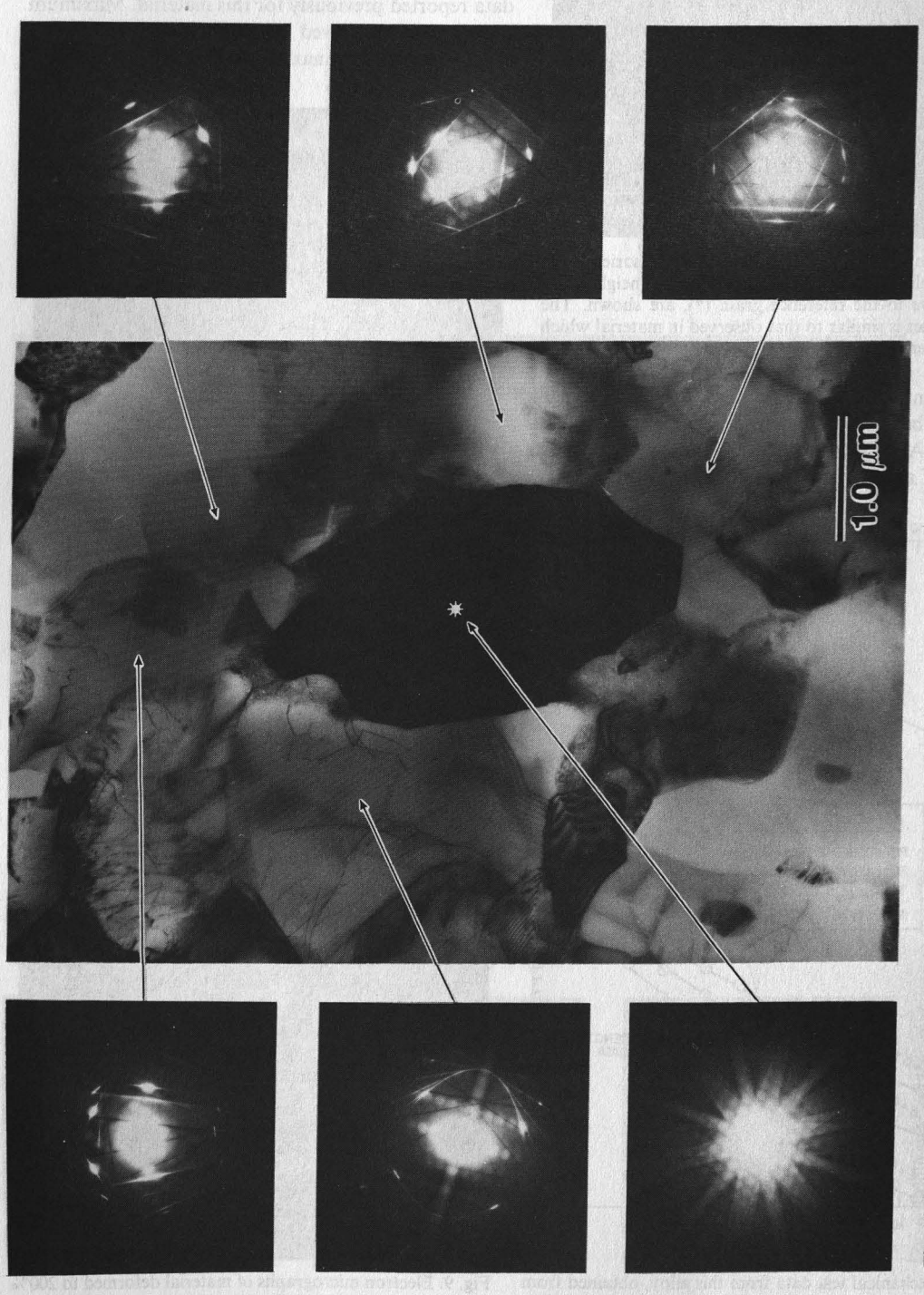

Fig. 10. Bright field electron micrograph and CBED patterns from the gage section of the superplastically deformed material (Fig. 9) showing the grains to be randomly oriented. The reference grain (*) is oriented with [011] parallel to *B*.

and the material behaves in a superplastic manner from the onset of deformation. The maximum m-value obtained is 0.45 and is observed at the smallest strain evaluated, 0.02. The micrographs in Fig. 9 were obtained from the gage section of a sample deformed 100% (a strain less than the fracture strain) at a strain-rate of $1.7 \times 10^{-2}\,s^{-1}$ (a strain-rate near that of peak ductility). The most noticeable feature is that, although the grain size has not increased appreciably, the grain shapes are much less equiaxed, Fig. 9(b). The weak beam micrograph, Fig. 9(c), shows that the dislocation density within grains is considerable. The distorted shape of the β precipitates, which contain evidence of deformation by slip, suggests that they have deformed during the tension test. A misorientation study, Fig. 10, reveals that the boundary angles have increased appreciably when compared to the data from the grip section (Fig. 6). The results are summarized in Fig. 11, which illustrates clearly that the average boundary misorientation is now 10–30°.

The data from Figs 3, 6 and 10, when plotted on a standard stereographic triangle, Fig. 12, conveniently demonstrate the extent to which boundary misorientations have increased. The misorientations between the reference grain, oriented on [011], and the adjacent grains are less than 10° in material which has experienced static annealing only but substantially greater than 10° in deformed material, i.e. annealed and then strained. This may be interpreted as evidence that the development of boundary misorientations is enhanced by the superplastic deformation process.

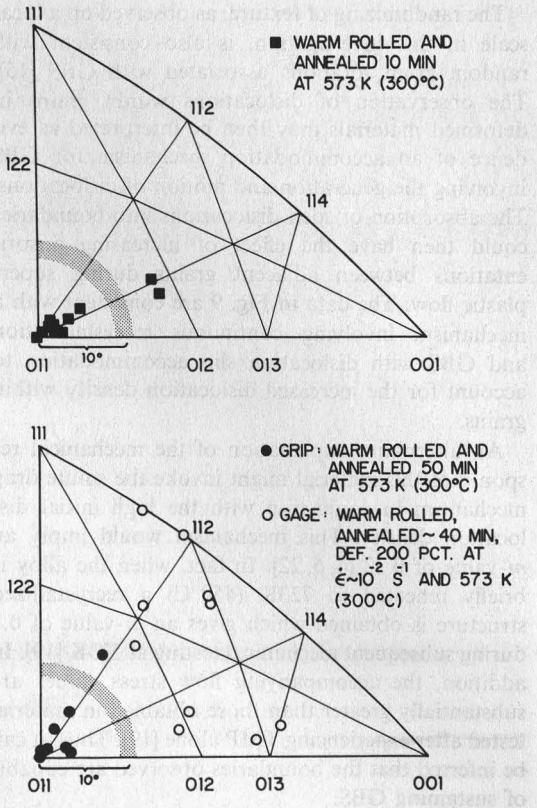

Fig. 12. Stereographic triangles containing the data from Figs 3, 6 and 10; the variation in orientations of the neighboring grains relative to the respective reference grains (oriented with [011] parallel to B) is plotted. Annealing only results in the majority of neighboring grains remaining within 10° of the reference grain whereas deformation to 100% strain results in much larger misorientations.

4. DISCUSSION

The results of the annealing experiments to simulate warm-up to the elevated test temperature reveal that the high dislocation density observed in the as-rolled material diminished rapidly. The TEM studies show that boundaries, with misorientations of 2–7°, form as a consequence of dislocation rearrangement alone during static annealing. Furthermore, there is no evidence to suggest a recrystallization mechanism based on nucleation and growth of new grains with accompanying high-angle boundary migration.

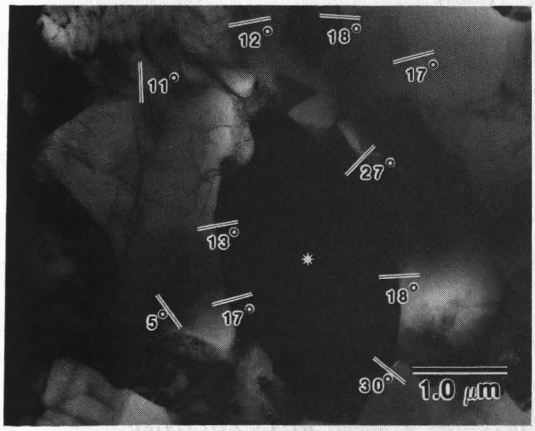

Fig. 11. Summary of the data from Fig. 10; the boundary misorientations have increased substantially (10–30°) when compared with material which has been annealed only (Fig. 7).

These boundary misorientations fall in a regime regarding which there is controversy [15, 21] as to whether they are subgrain or grain boundaries. The values obtained are low compared with those commonly associated with recrystallized grain structures but they are significantly greater than those observed in recovered subgrain structures. Examination of the mechanical property data reveals that the alloy, when processed by this TMP, behaves like a fine-grained superplastic material. The m-value of 0.45 is close to the value (0.5) ascribed to superplastic deformation involving GBS as the dominant mechanism. The fact that the misorientations between grains are low initially (2–7°) and increase substantially during deformation (10–30°) suggests that the boundaries are behaving as high-angle boundaries even with misorientations less than 10° at the onset of deformation.

The randomizing of texture, as observed on a local scale in this investigation, is also consistent with random grain rotations associated with GBS [15]. The observation of dislocations within grains in deformed materials may then be interpreted as evidence of an accommodation mechanism for GBS involving the generation and motion of dislocations. The absorption of such dislocations into boundaries could then have the effect of increasing misorientations between adjacent grains during superplastic flow. The data in Fig. 9 are consistent with a mechanism involving continuous recrystallization and GBS with dislocation slip accommodation to account for the increased dislocation density within grains.

An alternative explanation of the mechanical response of this material might invoke the solute drag mechanism in conjuction with the high initial dislocation density. This mechanism would imply an m-value of 0.33 [4, 6, 22]. In fact, when the alloy is briefly reheated to 723K (450°C) a recrystallized structure is obtained which gives an m-value of 0.3 during subsequent mechanical testing at 573K [19]. In addition, the accompanying flow stress values are substantially greater than those obtained in material tested after experiencing TMP alone [19]. Thus, it can be inferred that the boundaries observed are capable of sustaining GBS.

The results reported by Nes [15] were obtained using a Al–Cu–Zr (SUPRAL) alloy at considerably higher temperatures ($\sim$723K), that is $0.9T_m$. These are temperatures at which rapid grain growth would normally be expected to occur, necessitating a uniform dispersion of Al_3Zr to inhibit microstructural coarsening [7, 13]. The TMP used in this investigation but applied to a binary Al–Mg alloy with the same Mg content, results in material which does not exhibit a superplastic response. This is attributed to rapid microstructural coarsening at 573K because the β phase distribution alone is too coarse to stabilize the grain size. The Zr addition in the present alloy is insufficent to produce a fine Al_3Zr dispersion, nonetheless the Zr addition has resulted in retardation of grain coarsening facilitating a superplastic response at 573K.

Superplastic ductilities have been attributed to a combined precipitation and recrystallization mechanism in materials with large potential volume fractions of second phase [15, 21]. The grain refinement necessary for superplasticity has been reported to be a result of the combination of these processes [23, 24]. In this work, the TMP temperatures employed are the same as the superplastic deformation temperature and it has been shown previously that the β phase reaches its equilibrium volume fraction during TMP [25]. Clearly, there can be little or no further precipitation of the β phase during superplastic deformation and thus, the grain refinement achieved cannot be attributed to such a mechanism.

5. CONCLUSIONS

1. Continuous recrystallization is the mechanism responsible for converting a high dislocation density structure into a fine-grained structure capable of sustaining low temperature, high strain-rate deformation.

2. Stress/strain-rate data show that the material exhibits a superplastic response from the onset of deformation with an m-value of 0.45.

3. The m-value obtained reflects GBS as the dominant deformation mechanism in the maximum ductility region, as opposed to a solute drag based mechanism.

4. Boundary misorientations between adjacent grains increase rapidly during superplastic deformation.

5. The material is capable of a superplastic response while exhibiting a microstructure consisting of average boundary misorientations of less than 10°.

Acknowledgements—Financial support for this research was provided by the U.S. Naval Air Systems Command, with Dr Lewis Sloter as program monitor. The use of the Phillips EM430 at the Center for Microanalysis of Materials, University of Illinois, Urbana, Ill. is also gratefully acknowledged.

REFERENCES

1. B. M. Watts *et al.*, *Metal Sci. J.* **6,** 189 (1976).
2. C. H. Hamilton, C. C. Bampton and N. E. Paton, *Proc. Conf. Superplastic Forming of Structural Alloys* (edited by N. E. Paton and C. H. Hamilton), p. 173. T.M.S.-A.I.M.E., Warrendale, Pa (1982).
3. J. W. Edington, *Metall. Trans.* **13A,** 703 (1982).
4. R. C. Gifkins, *Proc. Conf. Superplsatic Forming of Structural Alloys* (edited by N. E. Paton and C. H. Hamilton), p. 3. T.M.S.-A.I.M.E., Warrendale, Pa (1982).
5. W. D. Nix, *Proc. Symp. Superplastic Forming* (edited by S. P. Agarwal), p. 3. Am. Soc. Metals, Metals Park, Ohio (1984).
6. O. D. Sherby and J. Wadsworth, *Proc. Conf. Deformation Processing and Microstructure* (edited by G. Krauss), p. 355. Am. Soc. Metals, Metals Park, Ohio (1984).
7. J. A. Wert, *Proc. Conf. Microstructural Control in Aluminum Alloys* (edited by E. H. Chia and H. J. McQueen), p. 67, T.M.S.-A.I.M.E., Warrendale, Pa (1986).
8. D. A. Woodford, *Trans. Am. Soc. Metals* **62,** 291 (1969).
9. M. A. Burke and W. D. Nix, *Acta metall.* **33,** 1267 (1981).
10. J. A. Wert *et al.*, *Metall. Trans.* **12A,** 1267 (1981).
11. J. Wadsworth, T. G. Nieh and A. K. Mukherjee, *Proc. Int. Conf. Aluminum Alloys—Physical and Mechanical Properties* (edited by E. A. Starke Jr and T. H. Sanders), p. 1239. EMAS, Warley, West Midland, U.K. (1986).
12. F. Haessner, *Recrystallization of Metallic Materials* (edited by F. Haessner), p. 1. Dr Riederer, Stuttgart (1978).
13. B. M. Watts *et al.*, *Metal Sci. J.* **6,** 198 (1976).
14. E. Nes, *J. Mater. Sci.* **13,** 2052 (1978).
15. E. Nes, *Superplasticity* (edited by B. Baudelet and M. Suery), p. 7.1. Editions du C.N.R.S., Paris (1985).
16. R. H. Bricknell and J. W. Edington, *Metall. Trans.* **10A,** 1257 (1979).

17. T. R. McNelley, E.-W. Lee and M. E. Mills, *Metall. Trans.* **17A,** 1035 (1986).
18. E.-W. Lee, T. R. McNelley and A. F. Stengel, *Metall. Trans.* **17A,** 1043 (1986).
19. E.-W. Lee and T. R. McNelley, *Mater. Sci. Engng J.* In press.
20. T. R. McNelley, E.-W. Lee and A. Garg, *Proc. Int. Conf. Aluminum Alloys—Physical and Mechanical Properties* (edited by E. A. Starke Jr and T. H. Sanders), p. 1269. EMAS, Warley, West Midlands, U.K. (1986).
21. A. R. Jones, *Proc. Sem. Grain Boundary Structure and Kinetics*, p. 379. Am. Soc. Metals, Metals Park, Ohio (1980).
22. J. Weertman, *J. appl. Phys.* **28,** 1185 (1957).
23. A. K. Ghosh and R. Raj, *Acta metall.* **29,** 607 (1981).
24. E. Hornbogen, *Proc. Int. Symp. Recrystallization and Grain Growth in Multi-phase and Particle Containing Materials* (edited by N. Hansen, A. R. Jones and T. Leffers), p. 199. Risø National Laboratory, Roskilde, Denmark (1980).
25. T. R. McNelley and A. Garg, *Scripta metall.* **18,** 917 (1984).